Am J Transl Res 2015;7(6):1140-1151
www.ajtr.org /ISSN:1943-8141/AJTR0006647

Original Article

DLAT subunit of the pyruvate dehydrogenase complex is upregulated in gastric cancer-implications in cancer therapy

Wen Quan Jonathan Goh[1], Ghim Siong Ow[3], Vladimir A Kuznetsov[2,3,4], Shirly Chong[1], Yoon Pin Lim[1,2,3]

[1]Department of Biochemistry, Yong Loo Lin School of Medicine, 117545, Singapore; [2]NUS Graduate School for Integrative Sciences and Engineering, National University of Singapore, 117456, Singapore; [3]Bioinformatics Institute, Agency for Science and Technology, 138671, Singapore; [4]School of Computing Engineering, Nanyang Technological University, 639798, Singapore

Received April 18, 2015; Accepted June 9, 2015; Epub June 15, 2015; Published June 30, 2015

Abstract: An iTRAQ-based tandem mass spectrometry approach was employed to relatively quantify proteins in the membrane proteome of eleven gastric cancer cell lines relative to a denominator non-cancer gastric epithelial cell line HFE145. Of the 882 proteins detected, 57 proteins were found to be upregulated with > 1.3-fold change in at least 6 of the 11 cell lines. Bioinformatics analysis revealed that these proteins are significantly associated with cancer, cell growth and proliferation, death, survival and cell movement. The catalogue of membrane proteins presented that are potential regulators/effectors of gastric cancer progression has implications in cancer therapy. DLAT, a subunit of the pyruvate dehydrogenase complex, was selected as a candidate protein for further studies as its function in gastric cancer has yet to be established. SiRNA studies supported a role of DLAT in gastric cancer cell proliferation and carbohydrate metabolism, reprogramming of which is a hallmark of cancer. Our study contributes to recent interest and discussion in cancer energetics and related phenomena such as the Warburg and Reverse Warburg effects. Future mechanistic studies should lead to the elucidation of the mode of action of DLAT in human gastric cancer and establish DLAT as a viable drug target.

Keywords: Gastric cancer, proteomics, membrane, DLAT, proliferation, cancer energetics

Introduction

Globally, gastric cancer accounts for 8% of total cancer cases and 10% of total deaths, with the majority of these cases occur in the developing countries [1]. A multifactorial model of carcinogenesis in gastric cancer is currently favored: external factors such as diet and infection with *Helicobacter pylori* [2] or co-carcinogens with internal factors such as genetic susceptibility or molecular dysregulation are linked [3]. Management of external factors has been the main cause of recent decline in gastric cancer incidence rates [1], but various authors caution that external, non-molecular risk factors such as *H. pylori* infection [4], high intake of salt and smoked food [5] have been shown to be neither sufficient nor necessary to cause gastric cancer. Survival rates for gastric cancer also remain low [6].

While controlling external factors can help in the management of gastric cancer, genetic alterations, and the resultant aberrant structure or expression of proteins are believed to be the underlying cause of gastric carcinogenesis [3, 7-9]. Some previously mentioned associations are between E-cadherin and familial gastric cancer [10] and c-Met and invasiveness [11]. Other proteins associated with neoplasticity are p53, APC [3], and altered Hedgehog signaling [12-16]. Molecular cancer markers and drug targets for diagnosis and treatment are still needed. With the advent of functional proteomics and mass-throughput systems of analysis, many new proteins as potential diagnostic, prognostic, predictive factors and drug targets can be elucidated.

Cellular membranes are important signal transduction platforms of cells, providing the first

point of contact with external environment such as the plasma membrane. Membrane lipids can also be modified to act as second messengers, as in the case of IP3, or to recruit cytosolic proteins to the membrane to trigger a signaling cascade. As such, the membrane proteome could be a rich source of molecular regulators and effectors of cellular transformation and progression. In this study, we hypothesized that the patho-physiological functions of the membrane proteins in gastric cancer cells are associated with alterations in cell growth and certain hallmarks of cancer. To test this hypothesis, we compared the expression levels of proteins found in the membrane fraction of 11 gastric cancer cell lines to non-cancerous gastric epithelial cell line, HFE145 using the isobaric tag for relative and absolute quantification (iTRAQ) approach [17].

The aim of this study is to investigate novel gastric cancer associated proteins and to establish them as potential drug targets for the treatment of gastric cancer through functional studies. Dihydrolipoamide S-acetyltransferase (DLAT), a mitochondrial protein involved in glucose metabolism, was up-regulated in gastric cancer cell lines. Its function in gastric cancer cell growth and proliferation as well as its association with altered energy metabolism in cancer were investigated.

Materials and methods

Chemicals and reagents

IGEPAL, Triton X-100, DMSO, NaCl, sodium fluoride, EGTA, EDTA and sodium orthovanadate were purchased from Sigma Aldrich (St Louis, MO). Protease inhibitor cocktails were obtained from Roche (Nutley, CA). EDTA. Transfection reagent JetPRIME™ was supplied by Polyplus-transfection Inc. (New York, USA).

Antibodies

Anti-DLAT was obtained from Abcam (Cambridge, UK). Actin-HRP antibody was obtained from Santa Cruz Biotechnology (Santa Cruz, CA), while anti-mouse IgG and anti-rabbit IgG HRP conjugates was obtained from Sigma Aldrich (St Louis, MO).

Cell culture and lysis

Ten human gastric cancer cell lines (AGS, TMK-1, NUGC3, NUGC4, SNU484, MKN45, KatoIII, SGC7901, SNU5 and SCH) were cultured in RPMI1640 medium containing 10% fetal bovine serum and 1% penicillin/streptomycin, non-cancerous gastric epithelial cell line (HFE145) and one of the gastric cancer cell line (HGC27) were cultured in DMEM medium containing 10% fetal bovine serum and 1% penicillin/streptomycin. The cells were incubated at 37°C in a humidified atmosphere containing 5% CO_2 until a cell confluence of 80% for further studies.

Membrane protein extraction

The cells were scraped in 1 ml of fractionation buffer (10 mM Tris. HCl, pH 7.4, 1 mM EGTA, 1 mM EDTA, 2 mM $MgCl_2$, 10 mM KCl, 100 mM NaF, 10 mM sodium pyrophosphate, 1 mM sodium vanadate, protease inhibitor cocktails) and kept at 4°C for 30 min. The cells were lysed by 15 strokes in a Dounce homogenizer, and the lysate was then layered on fractionation buffer with 1 M sucrose and centrifuged at 1,500 × g for 10 min. Approximately 1 ml of the supernatant above the sucrose cushion was removed and centrifuged at 150,00 × g for 30 min at 4°C. The supernatant (cytosolic fraction) was discarded. The membrane pellet was washed once with fractionation buffer, resuspended with the same buffer with the addition of 0.5% IGEPAL and Triton × 100, and centrifuged again at 150,00 g for 30 min at 4°C. The supernatant was collected as the membrane fraction.

Labeling of sample with iTRAQ reagents

Proteins from each cell line were subjected to iTRAQ labeling according to manufacturer's protocol (Applied Biosystems, Framingham, MA). Briefly 200 µg of protein was reduced using 2 µL of Reducing Reagent at 37°C for an hour. Subsequently 1 µL of Cysteine-Blocking Reagent was added for cysteine blocking and was incubated at room temperature for 10 minutes. A total of 4 µg of trypsin was used for each cell line for digestion in accordance with the ratio of 1 µg of trypsin to 50 µg of protein sample. Subsequently, the samples were incubated overnight at 37°C. Isopropanol was used to dissolve each iTRAQ Reagent and the content in one sample tube was transferred to one iTRAQ Reagent vial. The tubes were incubated at room temperature for 1 hour after vortex.

Fractionation of peptides by strong cation exchange (SCX) HPLC

The iTRAQ labeled peptides were dissolved in Buffer A which contained 5 mM KH2PO4 and 25% ACN (pH 2.7). Fractionation of peptides was performed using 1260 Infinity High Performance Liquid Chromatography (Agilent Technologies, USA), using a PolySULFOETHYL ATM column, 200 × 4.6-mm, 5 μm, 200-Å (PolyLC Inc.). A 60 minute step gradient was used where the gradient started with 100% of Buffer A for 5 minutes, followed by a ramp from 5 to 21% of Buffer B (5 mM KH2PO4, 25% ACN, 500 mM KCl, pH 2.7) for 35 minutes, then ramping from 30 to 100% of Buffer B for 15 minutes and maintained at 100% of Buffer B for 5 minutes. The fractions obtained were lyophilized in a vacuum concentrator and subsequently cleaned via a C-18 cleanup using C18 Discovery DSC-18 SPE column (100 mg capacity, Supelco, Sigma-Aldrich). The cleaned fractions were again lyophilized and then stored at -20°C prior to mass spectrometric analysis.

Mass spectrometric analysis

Each cleaned peptide fraction was dissolved in 35 μL of Buffer A which contained 2% ACN in 0.1% formic acid. 10 μL of each sample was injected into the nano-LC-ESI-MS/MS system by an autosampler for each analysis. Mass spectrometry was performed by QStar Elite Hybrid ESI Quadrupole time of flight tandem mass spectrometer (Applied Biosystems, Framingham, MA) coupled to an online capillary liquid chromatography system (Tempo nLC, Applied Biosystems, Framingham, MA). The column used to separate the peptide mixture was a PepMap C-18 RP capillary column (Dionex, The Netherlands). Peptide mixture separation was conducted at 0.3 μL/min, on a 125 minute gradient. The gradient started with 4% of Buffer B (98% ACN in 0.1% formic acid) and 96% of Buffer A for 3 minutes. Two ramping gradients of 4% of Buffer B in 7 minutes, 10 to 35% of Buffer B for 55 minutes and 35 to 100% of Buffer B for 25 minutes followed by a hold at 100% of Buffer B for 15 minutes and 96% of Buffer A for 20 minutes. The mass spectrometer was set in the positive ion mode, with a selected mass range of 300-1800 m/z. The time of summation of MS/MS events was adjusted to 2 seconds. Two charged peptides with the highest abundance above a 20 count threshold were chosen for MS/MS and dynamically excluded for 30 seconds with a mass tolerance within the range of ± 50 mDa. Protein identification and quantification for iTRAQ samples were carried out by importing the data files (*.wiff) into ProteinPilotTM software and analyzed using the Paragon algorithmTM (version 2.0; Applied Biosystems, MDS-Sciex). The search was performed against the International Protein Index (IPI) human (version 3.87, date of release: September 2011). The search parameters allowed cysteine modification of MMTS and biological modifications pre-defined in the software. The detected protein threshold (unused protscore (conf)) in the software was set to 1.3 to achieve 95% confidence.

Whole cell lysate extracts

Cells were rinsed with ice-cold phosphate buffered saline (PBS) before lysis on ice for protein extraction using non-ionic denaturing detergent (NID) lysis buffer [50 mM Tris-HCl (pH 7.5), 0.5% IGEPAL, 0.5% Triton X-100, 150 mM sodium chloride, 1 mM EDTA, 50 mM sodium fluoride, 1 mM sodium orthovanadate and protease inhibitor cocktail]. Cell debris was removed from the lysates by centrifuging at 4°C, 14,000 rpm for 10 minutes. Protein concentrations were subsequently determined using a Bicinchoninic Acid Assay (BCA) kit (Thermo Fisher Scientific, Rockford, IL) as per manufacturer's instructions. The absorbance was measured at 562 nm using a microplate reader.

Meta-analysis

Microarray data which profiles gastric cancer tumors was accessed from Gene Expression Omnibus (GEO) database [18]. Specifically, the following datasets of gastric cancers were downloaded: GSE27342, GSE13911 and GSE33651. In GSE27342, a total of 160 samples comprising of paired tumor and adjacent normal tissues from 80 gastric cancer patients were previously analyzed using Affymetrix Human Exon 1.0 ST Array as previously described [19, 20]. In GSE13911, a total of 69 samples with 38 tumor samples from gastric cancer and 31 adjacent normal tissues were previously profiled via microarray analysis as described [21]. In GSE33651, 40 gastric tumor tissue samples and 12 normal gastric tissue samples were analyzed as previously described [22]. Differential expression analyses between

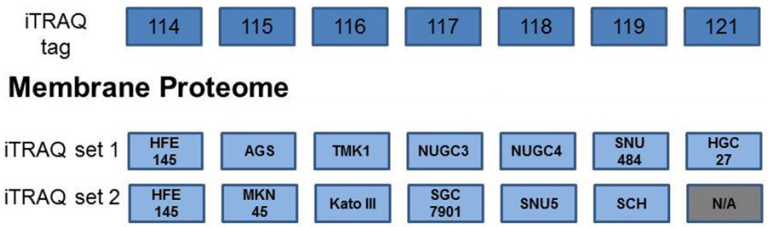

Figure 1. Experimental design for iTRAQ-based relative quantification of membrane proteins in a panel of gastric cancer cell lines compared to HFE145 non-cancerous cell line.

the normal and tumor tissues in each of the dataset were performed via non-parametric Mann-Whitney test. In addition, for datasets GSE27432 and GSE13911 which contain paired adjacent normal-tumor sample, differential expression analysis of the paired expression data were performed via Wilcoxon signed-rank test. In both Mann-Whitney and Wilcoxon signed-rank tests, the null hypothesis is that there is no significant difference in expression between the tumor samples and normal samples. All *p*-values are two-sided. A *p*-value < 0.05 is required to reject the null hypothesis. The statistical analysis was implemented in Python programming language and the scientific package (scipy). The figures were generated via the matplotlib plotting library.

SiRNA transfection

Following trypsinization, cells in suspension were transfected with 50 nM siRNA using the JetPRIME™ transfection reagent (Polyplus Transfection Inc.) according to the manufacturer's instructions. Cells were incubated for 48 hours to achieve maximum knockdown, and they were subsequently harvested for Western blot analysis or to perform functional assays. The siRNA sequences were purchased from Life Technologies (Thermo Fisher Scientific, Rockford, IL) under the following product codes targeting the respective exons: DA sequence (HSS102785, targeting exon 1): 5'-UCGCAACAGCGUGACUACAGGGUA-3'; DB sequence (HSS102786, targeting exon 13): 5'-GGAUAAACUGGUCCCUGCAGAUAAU-3'. Luc control siRNA #5270471 was purchased from Life Technologies, USA.

Growth and proliferation assay

At intervals of 24 hours, different populations of cells which all began from a cell count of 2000 were subjected to a Cell Titer 96® AQueous Non-Radioactive Cell Proliferation Assay according to manufacturer's instruction. In short, PMS and MTS solution were mixed in a ratio of 100 µl PMS to 2.0 ml of MTS Solution. 20 µl of the MTS/PMS solution was added to each well containing 100 µl of cells in culture medium. The plate was incubated for 1-4 hours at 37°C in a humidified, 5% CO_2 atmosphere. Absorbance was recorded at 490 nm using a microplate reader. Statistical analysis was performed using unpaired one-tailed Student's t-test.

Pyruvate quantification

These reagents are mixed together in these final concentrations at a buffering pH of 7.4: NADH-0.25 µM, KH2P04-0.1 M, LDH-1.3 u/mL. This master mix is mixed with cell lysate standardized to a weight of 120 ng of protein, immediately before fluorescence of NADH was measured over time at 535/464 nm with a plate reader. The bigger the drop in fluorescence, the more pyruvate is present. All cell lysate samples were standardized to a weight of 120 ng of protein and results were obtained from 2 biological replicates, with 3 technical replicates within each biological replicate. Internal pyruvate standards were added to allow conversion from relative fluorescence units/min to absolute amounts of pyruvate. As a kinetics assay, the initial velocity (RFU/min) is taken instead of the endpoint for practical reasons. The R^2 value of the standards is more than 0.95 and the standards are deemed trustworthy to give an absolute quantification. Statistical analysis was performed using unpaired one-tailed Student's t-test.

Gene ontology analysis

Gene ontology analysis was performed via the bioinformatics software Ingenuity Pathway Analysis (IPA). The statistical value of the enrichment of our genes in various gene ontology terms was calculated via Fisher's exact test which is based on hypergeometric distribution. *P*-values reported by IPA are right-tailed, and test the null hypothesis that there is no over-

Table 1. List of 57 proteins that we found to be aberrantly up regulated in at least 6 gastric cancer cell lines compared to HFE145 non cancer cells

	AGS: HFE	TMK1: HFE	NUGC3: HFE	NUGC4: HFE	SNU484: HFE	HGC27: HFE	MKN45: HFE	KatoIII: HFE	SGC7901: HFE	SNU5: HFE	SCH: HFE	Freq up
PRDX1	1.559	1.917	1.480	1.466	1.856	1.409	1.363	1.203	2.129	1.780	2.030	10
EEF1B2	1.390	1.924	1.432	1.124	1.707	1.343	2.189	1.465	1.872	1.736	1.458	10
MDH2	1.015	1.568	1.328	2.143	1.881	1.570	1.645	2.005	1.209	2.665	1.529	9
S100A14	1.819	4.184	2.863	5.327	1.063	0.972	1.421	3.592	2.086	2.217	2.245	9
SLC1A5	1.487	1.551	1.440	1.401	0.913	1.549	1.000	1.896	1.447	1.420	1.238	8
HEXB	1.883	1.366	0.947	1.926	3.262	1.459	1.124	1.938	1.363	1.377	1.172	8
SFN Isoform 1	2.282	1.384	1.859	2.233	0.894	0.938	2.163	1.834	2.616	2.980	0.945	8
ECH1	1.601	2.605	1.023	1.831	2.463	1.045	2.033	1.845	1.640	1.880	1.190	8
HYOU1	1.741	2.197	1.013	1.458	1.656	1.399	1.818	2.329	0.967	0.955	1.453	8
KRT18	2.083	1.531	3.442	1.573	0.908	0.873	2.782	1.876	1.612	1.112	2.107	8
HNRNPK	1.861	1.185	1.348	0.867	1.305	1.738	1.479	1.325	1.428	1.083	1.431	8
LMNA	1.308	1.187	1.530	0.963	1.713	1.803	1.807	1.680	1.171	1.632	1.985	8
PPIA	1.184	1.564	1.179	1.597	1.433	1.608	1.900	1.289	1.463	2.083	1.375	8
ANXA1	0.886	0.953	1.375	2.290	3.053	1.779	2.539	1.183	1.575	2.377	1.341	8
SLC7A5	1.365	6.086	1.517	0.733	0.822	1.627	1.006	3.759	3.471	1.613	2.960	8
DLAT	0.953	1.855	1.304	0.969	1.883	1.317	1.191	2.243	1.407	2.017	1.701	8
C14orf156	1.243	1.420	1.240	1.679	1.597	1.342	1.071	1.414	1.349	1.834	1.335	8
GCSH	1.410	3.765	1.792	1.797	3.451	1.842	1.355	1.953	1.863	2.727	7.052	8
KRT8	2.641	1.147	3.118	2.107	0.827	0.858	3.119	1.886	1.581	1.543	2.763	8
HSPA9	1.111	1.936	1.193	1.580	1.666	1.227	1.400	1.906	1.582	2.151	1.520	8
NDUFAB1	1.001	1.300	1.094	1.826	1.561	1.086	1.809	1.890	1.392	2.148	1.307	8
ECHS1	1.190	1.395	0.940	2.421	1.868	0.814	1.565	1.852	1.337	1.991	0.968	7
C1QBP	1.058	1.397	1.274	2.193	1.841	1.100	1.662	1.901	1.350	1.512	1.212	7
HNRNPL	1.628	1.079	1.385	0.999	1.325	1.689	1.706	1.331	1.186	1.185	1.619	7
HNRNPA2B1	1.619	1.019	1.529	0.965	1.314	1.539	1.656	1.442	1.104	1.054	1.489	7
PABPC1	1.516	1.388	1.468	0.931	1.207	1.415	1.411	1.272	1.394	1.164	1.681	7
MRPL12	1.087	1.503	1.294	2.022	1.729	1.004	1.321	1.930	1.072	2.168	1.420	7
ACTN4	1.403	1.257	1.535	1.364	0.889	0.835	1.072	1.622	1.608	1.528	2.482	7
SERBP1	1.498	1.495	1.119	0.502	1.370	1.661	1.587	1.091	1.548	0.893	1.406	7
CORO1B	1.742	1.599	1.364	1.104	1.467	1.551	1.269	1.266	1.310	0.970	1.000	6
CAPRIN1	1.510	1.530	1.127	1.217	1.618	1.616	1.428	1.069	1.625	1.240	1.248	6
G3BP1	1.478	1.332	1.072	0.701	1.370	1.379	1.310	1.007	1.494	0.831	1.161	6
EIF3G	1.390	1.506	1.210	1.115	1.229	1.551	1.392	1.435	1.043	1.433	1.270	6
TXN	1.204	2.024	1.261	2.114	1.097	1.385	1.260	1.925	1.371	1.996	1.064	6
ETFB	0.761	1.559	0.948	1.613	1.185	0.997	1.497	1.586	1.361	1.670	1.114	6
HSPE1	1.027	1.062	1.326	3.060	1.195	1.010	1.406	1.571	1.367	2.217	1.075	6
ACAA2	0.782	1.450	1.046	1.110	1.873	1.097	1.459	2.794	1.413	1.473	1.233	6
TUFM	1.138	1.200	1.131	1.949	1.338	1.049	1.417	1.534	1.318	1.520	1.043	6
S100A4	0.851	5.493	1.101	1.105	0.861	1.556	5.874	1.427	1.662	2.381	0.877	6
KRT19	2.076	1.826	2.294	1.585	0.816	0.824	2.418	1.291	1.098	1.279	2.429	6
KHSRP	1.438	0.930	1.584	0.851	1.301	1.775	1.756	0.960	0.943	0.826	1.594	6
TPD52	1.105	1.555	1.576	1.070	1.437	1.680	1.581	1.343	1.331	0.969	1.799	6
ERP29	1.783	2.219	1.053	1.702	1.815	1.140	1.025	1.675	1.142	1.243	1.454	6
HSP90B1	1.602	1.699	0.903	1.443	1.718	0.911	1.050	1.582	1.051	0.943	1.346	6
VASP	1.741	2.384	1.254	1.228	2.409	0.921	2.325	1.263	1.746	1.074	1.337	6
SLC9A3R1	1.740	2.209	0.896	1.618	1.088	0.888	1.134	1.749	1.385	1.071	2.542	6
DYNLL1	1.216	1.339	1.355	1.285	1.374	1.240	1.345	1.200	1.220	1.345	1.428	6
HMGB2	1.143	0.711	1.289	1.549	1.433	1.383	1.579	1.249	0.934	1.515	1.670	6
FIS1	0.865	1.581	1.225	1.887	1.461	1.085	1.007	1.696	1.144	2.025	1.512	6
DLD	1.016	1.315	1.114	1.636	1.509	1.057	1.283	1.486	1.159	2.367	1.365	6
TFRC	0.851	1.190	1.113	1.849	1.376	1.309	1.103	1.337	1.145	1.854	1.366	6
ATP5D	0.766	1.269	1.095	1.631	1.695	1.312	1.212	1.452	1.112	1.302	1.302	6
SOD1	1.251	1.394	1.030	1.091	1.481	1.203	1.513	1.351	1.293	1.525	1.505	6

PHB	0.851	0.991	0.971	1.742	1.379	1.222	1.460	1.442	0.972	1.392	1.386	6
NPM1	1.321	1.259	1.148	0.824	1.209	1.552	1.664	1.236	2.810	1.373	1.823	6
DCI	1.050	1.241	1.021	1.890	1.490	1.273	1.137	2.314	1.687	1.916	1.556	6
HMGA1	0.926	1.082	2.925	0.686	1.965	1.253	1.627	1.752	1.241	1.923	2.104	6

Ratios highlighted in red indicate upregulation while ratios highlighted blue indicate downregulation. Ratios not highlighted means that they are either not statistically significant or did not satisfy the criteria for classifying proteins as up (≥ 1.3) or downregulated (≤ 0.77). Freq up refers to the number of gastric cancer cell lines in which each individual protein was found to be upregulated.

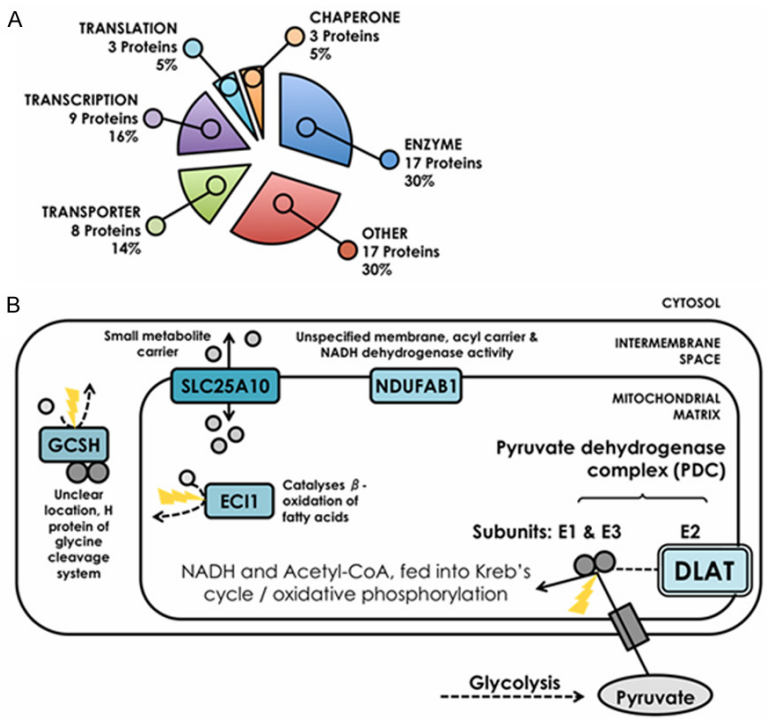

Figure 2. A. Ingenuity Pathway Analysis of 57 proteins that displayed aberrant expression in more than 6 gastric cancer cell lines into classical functions. B. Reported localization and function of 5 mitochondrial proteins found to be novel gastric cancer-associated proteins.

representation of our genes in a given biological process or function. To adjust for multiple hypothesis testing, the *p*-values were corrected via Benjamini-Hochberg method [23]. A corrected *p*-value cut-off of < 0.05 was set to identify statistical significant gene ontology terms.

Results

Detection of 882 proteins using iTRAQ-based LC/MS/MS across 11 gastric cancer cell lines

The experimental design of the study is shown in **Figure 1**. In set 1, proteins from HFE 145, AGS, TMK1, NUGC3, NUGC4, SNU484 and HGC27 were labeled with iTRAQ reagents 114, 115, 116, 117, 118, 119 and 121 respectively. In set 2, HFE145, MKN45, KatoIII, SGC7901, SNU5 and SCH, were labeled with iTRAQ reagents 114, 115, 116, 117, 118 and 119, respectively. The two sets of iTRAQ samples were then separately analysed and only common hits between the two sets of iTRAQ data were extracted and for further processing. The complete raw data of the iTRAQ-based relative quantification of 882 proteins detected across all cell lines used in this study, using HFE145 as a denominator, including error factor, *p*-value etc. is shown in Supplementary Table 1. As described in "Methods", only protein hits of 95% confidence and at least 2 unique peptides are included.

Analysis of the technical variation in our analytical systems has consistently been below 30% [24-27]. Hence, a 1.3-fold change cutoff (upper and lower range cut off were 1.3 and 0.77, respectively), was used to classify the protein expressions as up-regulated or down-regulated. Therefore, proteins with iTRAQ fold change (FC) ratios which are statistically significant ($P < 0.05$) and $FC \geq 1.3$ were considered to be up-regulated while those with iTRAQ $FC \leq 0.7$ were considered to be down-regulated. The results of the classification of 660 proteins into up or down regulated is shown in Supplementary Table 2 (proteins whose iTRAQ ratios are not statistically significant i.e., $P > 0.05$ are not included).

Bioinformatics of the gastric cancer membrane proteome

Out of the 882 common proteins, 505 (57.3%) proteins were up and down-regulated in one or

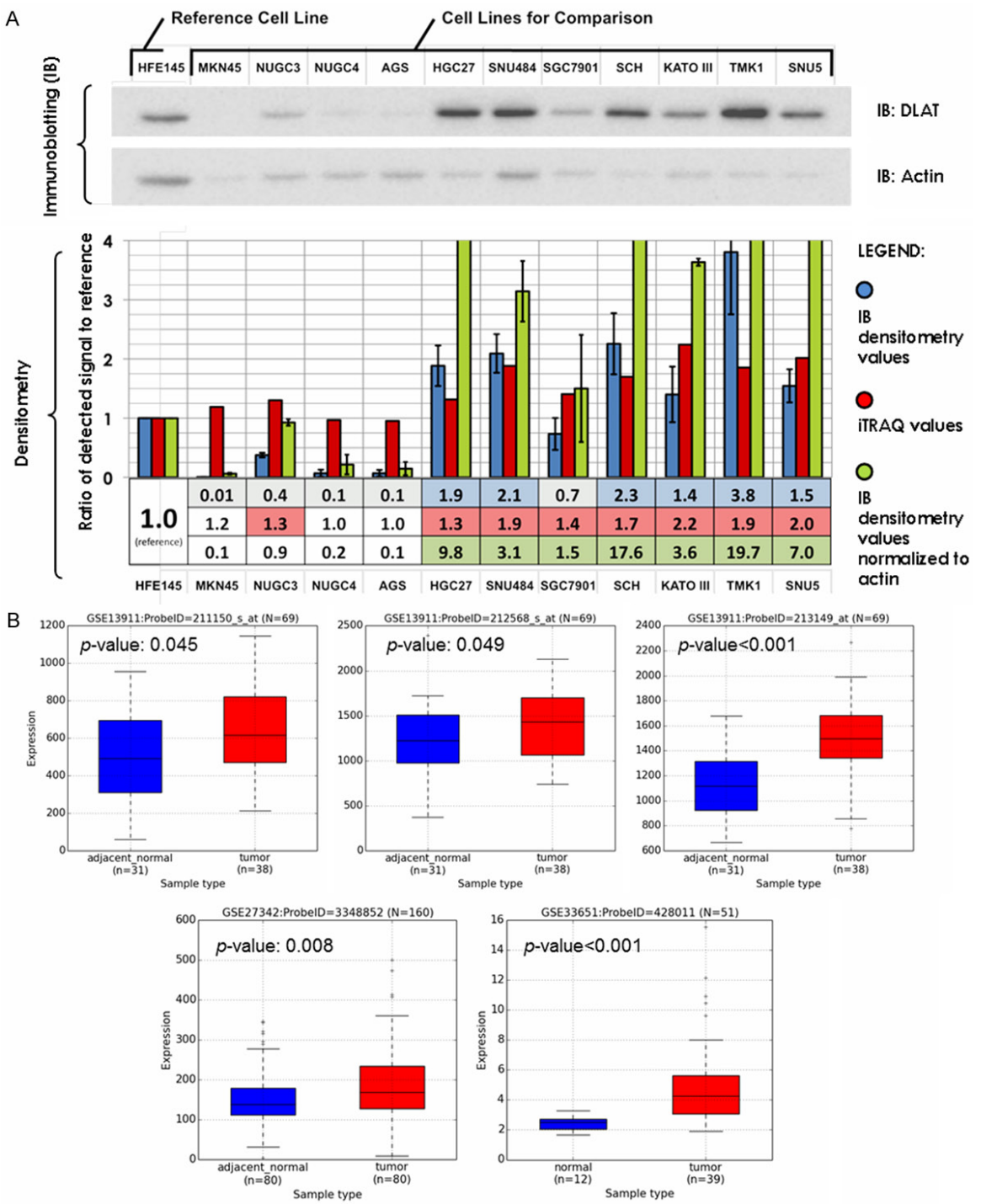

Figure 3. A. Upper panel, immunoblotting of DLAT across a panel of non-cancer HFE145 and gastric cancer cell lines. Lower panel, comparison of the densitometric readings obtained from immunoblotting with iTRAQ ratios. B. Meta-analysis of public databases on DLAT mRNA expression in gastric tumors versus normal tissues.

more of the eleven cell lines compared to HFE145. Of the 505 up-regulated proteins, 57 proteins were found to be up-regulated across more than half (6/11) of the cell lines (**Table 1**).

In order to ascribe biological meaning to the dataset, gene ontology analysis was conducted on the 57 commonly upregulated proteins using Ingenuity Pathway Analysis (IPA) soft-

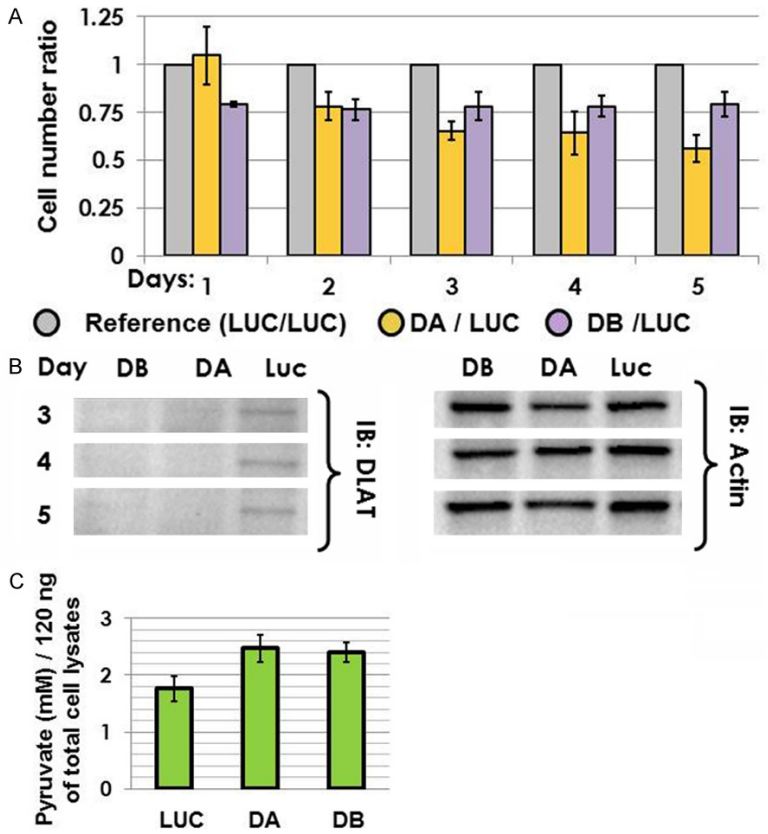

Figure 4. A. Growth and Proliferation assay of TMK1 cells transfected with control siRNA (Luc) or DLAT specific siRNA sequences DA and DB. B. Immunoblotting of DLAT in TMK1 cells transfected with control siRNA or DLAT-specific siRNAs after 3, 4 and 5 days of transfection. C. Quantification of pyruvate in DLAT knocked down and control cells following 3 days of transfection.

ware. We focused on up-regulated proteins due to our interest in potential oncogenes and drug targets. The major group comprises of drugable proteins with enzymatic activities representing 30% of the 57 proteins (**Figure 2A**). Next, we performed gene ontology functional enrichment analysis via IPA software (see methods). Classification of proteins into their respective functional classes is provided in Supplementary Table 3. We also conducted a literature review on these proteins as we were interested to identify novel cancer-associated proteins. The results revealed 5 proteins which also happened to be mitochondrial or mitochondrion-associated proteins: SLC25A10, GSCH, DLAT, NDUFAB1, ECI1 (**Figure 2B**). The presence of these mitochondrial proteins with a relatively strong up-regulation is interesting because, as an organelle, the mitochondrion is related to 2 hallmarks of cancer, the reprogramming of cellular energetics and evading cell death [28].

Selection of DLAT as a candidate for further studies

DLAT is one of the 3 mitochondrial proteins that were found to be upregulated in 8 out of 11 gastric cancer cell lines. It is found in the inner mitochondrial membrane and plays a role in the breakdown of pyruvate into Acetyl CoA and has not been previously linked to cancer. DLAT is the subunit E2 of the pyruvate dehydrogenase complex (PDC). PDC is an enzyme close to a key junction in the glucose catabolic pathway: catalysing the breakdown of pyruvate into acetyl-coA, using up NAD^+ and producing NADH. Regeneration of NAD^+ either happens in aerobic respiration via oxidative phosphorylation (OX-PHOS) or anaerobic lactic acid fermentation where lactate dehydrogenase converts pyruvate to lactate. While the latter normally occurs in differentiated cells in an anaerobic environment, in cancer cells it occurs even in oxygen, at high levels: the Warburg effect [29, 30]. Anaerobic glycolysis cycles around 100 times faster than the equivalent aerobic processes, which is possibly a selective advantage for tumors, as they grow quickly and have urgent ATP needs [31, 32]. DLAT, as part of the PDC complex and a link between glycolysis and the Krebs Cycle/OX-PHOS, is intuitively predicted to be down-regulated, either in presence or function, in cancer if the Warburg Effect is assumed. This is not the case according to the mass spectrometry/proteomics data. Hence, we proceeded to verify the upregulation of DLAT expression in gastric cancer cell lines.

The relative ratios of DLAT expression across the 11 cell lines as determined by iTRAQ-based method are bold and italicized in **Table 1**. To validate the mass spectrometry data, immunoblotting (IB) was performed on the cell lysates from these 11 cell lines. Actin was used as a loading control. Densitometry was then performed on the signals obtained from immu-

noblots using the BioRad imager system and ImageLab program. In general, both the IB and iTRAQ methods are consistent in reflecting the upregulation trend of DLAT in the gastric cell cell lines compared to HFE145 cells although the ratios generated by both methods are not the same, which is to be expected since they are 2 different analytical methods (**Figure 3A**). However, immunoblotting but not the mass spectrometric data revealed some gastric cancer cell lines to possess lesser DLAT than the non-cancer cells. This may reflect the limitation of the mass spectrometry system in computing relative quantification from peptides using a shotgun, bottom-up approach.

To examine the clinical relevance of DLAT in clinical gastric cancer, we performed meta-analysis on 3 public microarray data sets (GSE-13911-3 probes used; GSE27342-1 probe used and GSE33651–1 probe used). In all cases, DLAT mRNA level was found to be higher in gastric tumors compared to normal tissues (**Figure 3B**). The statistical significance of the differential expressions was evaluated via non-parametric Mann-Whitney test. In addition for GSE27342 and GSE13911, as the samples consist of paired adjacent normal-tumor tissues, we also performed paired analysis of differential expression via Wilcoxon signed-rank test (results not shown). The statistical significance of DLAT differential expression in GSE27342 improved slightly when evaluated by paired Wilcoxon signed-rank test. However for GSE13911, the statistical significance of the DLAT differential expression decreased slightly due to the removal of some unpaired samples from analysis. Therefore for consistency of presentation across the three studied datasets, only the *p*-values of the unpaired Mann-Whitney test were shown (**Figure 3B**). From the larger GSE27342 data set, which comprises 80 paired normal and tumor samples, 50 matched cases had DLAT expression higher compared to control exp of DLAT while in 30 matched samples, expression of DLAT in tumor was less than normal tissues. Taken together, the immunoblotting and meta-analysis data indicate that upregulation of DLAT occurs only to a subset of gastric cancers and supports the notion that gastric cancer is a heterogeneous disease, i.e. gastric cancer in different patients are genotypically diverse. This also reiterates the need for individualized medicine.

DLAT knockdown in TMK1 cells reduced cell proliferation

The functional role of DLAT in cancer has never been established. We therefore aim to test the hypothesis that silencing DLAT expression would be associated with a decrease in growth and proliferation. Since TMK1 had the highest DLAT expression amongst our 11 cell lines, it was chosen for functional studies following knock down of DLAT. Prior to functional studies, we characterized and optimized the knock down of DLAT using 3 different siRNA sequences (DA, DB and DC) over a concentration of 10, 25, 50 and 100 nM. 50 nM of siRNA was deemed to be optimal for knock down of DLAT; in addition, DA and DB were more effective in silencing DLAT expression than DC (data not shown).

One population of TMK1 was split into three subpopulations, which were transfected according to manufacturer's instructions with DA, DB, and LUC control siRNA sequences, respectively. At intervals of 24 hours, these three subpopulations which all began from a cell count of 2000 were subjected to a Cell Titer 96® AQueous Non-Radioactive Cell Proliferation Assay according to manufacturer's instruction. Relative ratios of transfected cell population numbers to control cells were then plotted. Three biological replicates and 3 technical replicates within each biological replicate were assayed.

When the various populations transfected with DA and DB were compared to LUC, we observed that the DA/LUC Ratio dropped steadily over the 5 days from 100% to about 50%, indicating an inhibition of proliferative capability relative to the negative control when DLAT was knocked down by DA (**Figure 4A**). A similar result was observed by the DB/LUC Ratio, although the ratios were constant at 0.8 and did not drop further. Effective silencing of DLAT expression was demonstrated following DLAT immunoblotting of the cell lysate generated on the 3rd, 4th, and 5th day (**Figure 4B**). It is unclear why different siRNAs against DLAT produced slightly different effects on the proliferation of gastric cancer cells. It is conceivable that DA sequence targets different DLAT variants/isoforms more effectively than the DB sequence. However, this postulation needs to be tested since our antibody could only detect 1 specific band in the cell lysates.

DLAT knockdown in TMK1 cells increased cellular pyruvate amounts

As DLAT is classically involved in the breakdown of pyruvate, the absence of DLAT should cause some level of pyruvate accumulation. Therefore, we next hypothesized that knockdown of DLAT would be associated with increased cell pyruvate levels. Due to inherent difficulty in directly measuring PDC activity, we opted to do a LDH activity assay on the cell lysates previously used in day three of the cell proliferation assay instead. This LDH activity assay mimics LDH activity in converting pyruvate to lactate with coenzyme NADH being used up in the process. In other words, the more the pyruvate in the cells, the lesser the amount of NADH would be detected. NADH was provided in excess in the assay so that it was not a limiting factor. Fluorescence of NADH was measured over time at 535/464 nm as mentioned in "Methods". Our results show that the pyruvate levels of both DA and DB were significantly higher than LUC on day three. DA > LUC, ($P = 0.00017$), DB > LUC ($P = 0.00012$) (**Figure 4C**). Hence, DLAT knock down resulted in a blockage in the conversion of pyruvate into Acetyl CoA, leading to accumulation of pyruvate in the cells.

Discussion

DLAT is the subunit E2 of the PDC complex in the catabolic glucose pathway. It has not been previously shown to be up-regulated in gastric cancer, but has one of the highest up-regulation ratios in some gastric cancer cell lines tested in this study. Due to re-emerging interest in cancer energetics, our laboratory investigated its possible role in gastric cancer. Knockdown of DLAT using siRNA reduced cell proliferation by approximately 20-45% that is associated with increased cellular pyruvate, presumably resulting in decrease in energy production through a blockage in the conversion of pyruvate to Acetyl CoA. Although our results support a functional role of DLAT in gastric cancer, it is unclear whether DLAT is a driver gene. To this end, future gain of function studies involving DLAT over-expression would be necessary. In addition, future immunohistochemistry studies on clinical samples would be necessary to establish the clinical relevance of DLAT in gastric cancer.

Our results can be further discussed in the light of the Warburg Effect, the Reverse Warburg effect, and anabolic metabolism. As earlier stated, DLAT is intuitively expected to be down-regulated if the Warburg Effect is assumed. This may indeed be the case in some gastric cancer cell lines in which DLAT was under-expressed compared to non-gastric cancer epithelial cells. However, our results also showed that DLAT was not only upregulated in a considerable number of gastric cancer cell lines, it also retained its classical function as a PDC subunit in gastric cancer. The observation that silencing DLAT resulted in increased pyruvate and decreased cancer growth/proliferation is contrary to the intuitive postulation of the Warburg effect: since much of ATP production occurs through the anaerobic pathway, down-regulation of the aerobic pathway should not be detrimental to the ATP production and hence growth of the tumor.

The Warburg effect, however, is well documented, with fludeoxyglucose (FDG)-positron emission tomography (PET) commonly used to accurately visualize tumors [29, 30]. An alternate explanation for the Warburg Effect can be considered with our results. Tumor cells have been previously shown to take up lactate for mitochondrial oxidative phosphorylation via monocarboxylate carriers [33]. It is thus posited that tumor-associated fibroblasts surrounding tumor microenvironment, rather than the tumors, are the cells taking up FDG and undergoing the Warburg effect [34]. In this scheme, the surrounding tumor microenvironment is thus induced by the tumor to undergo aerobic glycosis and feed the tumor lactate for hypothesized energy advantage or efficiency. This has been previously observed and is termed the Reverse Warburg effect [34].

In the literature, tumor hypoxia is said to place selection pressure on cells to depend on anaerobic metabolism and hence bring about the Warburg effect in surviving cells. There is, however, little explanation for cancerous cells exhibiting the Warburg effect in their organ of origin with high oxygenation such as leukemic cells or lung tumors [35]. An alternate explanation in the literature suggests that the Warburg effect could instead be an underlying effect of an overall inclination towards anabolism, (the production of building blocks such as pyruvate) rather than catabolism (the production of ATP) [29, 32]. Oncogenic mutations or genetic aberrations in the growth factor pathways during cellular transformation may cause an overall increase in glycolysis and hence the Warburg

effect to support anabolic growth. At the same time, enzymes in the oxidative phosphorylation pathways like DLAT may be upregulated to generate the energy required to support catabolic activities.

In conclusion, DLAT is upregulated in gastric cancer cells. Our data supported its classical function as an enzyme in the aerobic glucose catabolic pathway in at least some of the gastric cancer cell lines, catalyzing the conversion of pyruvate into Acetyl CoA, presumably to facilitate oxidative phosphorylation, ATP generation and catabolic reactions, which is likely to be as important as anabolic reactions in cancer growth. DLAT protein may act as one of the potential drug targets in the mitochondria, against which many therapeutic strategies have been designed for cancer treatment [36].

Acknowledgements

This study is funded by the National Medical Research Council, Ministry of Health, Singapore.

Disclosure of conflict of interest

None.

Abbreviations

DLAT, Dihydrolipoamide S-acetyltransferase; PDC, Pyruvate dehydrogenase complex; iTRAQ, isobaric tagging for relative and absolute quantification.

Address correspondence to: Lim Yoon Pin, Department of Biochemistry, Yong Loo Lin School of Medicine, National University of Singapore, MD4, Level 1.5 Science Drive 2, 117545 Singapore. Tel: 65-66011891; E-mail: bchlyp@nus.edu.sg

References

[1] Jemal A, Bray F, Center MM, Ferlay J, Ward E and Forman D. Global cancer statistics. CA Cancer J Clin 2011; 61: 69-90.

[2] Uemura N, Okamoto S, Yamamoto S, Matsumura N, Yamaguchi S, Yamakido M, Taniyama K, Sasaki N and Schlemper RJ. Helicobacter pylori infection and the development of gastric cancer. New Engl J Med 2001; 345: 784-789.

[3] Zheng L, Wang L, Ajani J and Xie K. Molecular basis of gastric cancer development and progression. Gastric Cancer 2004; 7: 61-77.

[4] Tsugane S and Sasazuki S. Diet and the risk of gastric cancer: review of epidemiological evidence. Gastric Cancer 2007; 10: 75-83.

[5] Roder DM. The epidemiology of gastric cancer. Gastric Cancer 2002; 5: 5-11.

[6] Ebert MP, Schandl L and Malfertheiner P. Helicobacter pylori infection and molecular changes in gastric carcinogenesis. J Gastroenterol 2002; 37: 45-49.

[7] Ebert MP, Yu J, Hoffmann J, Rocco A, Röcken C, Kahmann S, Müller O, Korc M, Sung JJ and Malfertheiner P. Loss of beta-catenin expression in metastatic gastric cancer. J Clin Oncol 2003; 21: 1708-1714.

[8] Fiocca R, Luinetti O, Villani L, Mastracci L, Quilici P, Grillo F and Ranzani G. Molecular mechanisms involved in the pathogenesis of gastric carcinoma: interactions between genetic alterations, cellular phenotype and cancer histotype. Hepatogastroenterology 2000; 48: 1523-1530.

[9] Tamura G, Yin J, Wang S, Fleisher AS, Zou T, Abraham JM, Kong D, Smolinski KN, Wilson KT and James SP. E-Cadherin gene promoter hypermethylation in primary human gastric carcinomas. J Natl Cancer Inst 2000; 92: 569-573.

[10] Huntsman DG, Carneiro F, Lewis FR, MacLeod PM, Hayashi A, Monaghan KG, Maung R, Seruca R, Jackson CE and Caldas C. Early gastric cancer in young, asymptomatic carriers of germ-line E-cadherin mutations. New Engl J Med 2001; 344: 1904-1909.

[11] Yokozaki H, Yasui W and Tahara E. Genetic and epigenetic changes in stomach cancer. Int Rev Cytol 2001; 204: 49-95.

[12] Ruiz i Altaba A. Hedgehog signaling and the Gli Altaba AR. Hedgehog Signaling and the Gli Code in Stem Cells, Cancer, and metastases. Sci Signal 2011; 4: pt9.

[13] Li X, Ma Q, Duan W, Liu H, Xu H and Wu E. Paracrine sonic hedgehog signaling derived from tumor epithelial cells: a key regulator in the pancreatic tumor microenvironment. Crit Rev Eukaryot Gene Expr 2012; 22: 97-108.

[14] Liu H, Gu D and Xie J. Clinical implications of hedgehog signaling pathway inhibitors. Chin J Cancer 2011; 30: 13.

[15] Nolan-Stevaux O, Lau J, Truitt ML, Chu GC, Hebrok M, Fernández-Zapico ME and Hanahan D. GLI1 is regulated through Smoothened-independent mechanisms in neoplastic pancreatic ducts and mediates PDAC cell survival and transformation. Genes Dev 2009; 23: 24-36.

[16] Robbins DJ, Fei DL and Riobo NA. The Hedgehog signal transduction network. Sci Signal 2012; 5: re6.

[17] Ross PL, Huang YN, Marchese JN, Williamson B, Parker K, Hattan S, Khainovski N, Pillai S, Dey S, Daniels S, Purkayastha S, Juhasz P, Martin S, Bartlet-Jones M, He F, Jacobson A and Pappin DJ. Multiplexed protein quantita-

tion in Saccharomyces cerevisiae using amine-reactive isobaric tagging reagents. Mol Cell Proteomics 2004; 3: 1154-1169.
[18] Barrett T, Suzek TO, Troup DB, Wilhite SE, Ngau WC, Ledoux P, Rudnev D, Lash AE, Fujibuchi W and Edgar R. NCBI GEO: mining millions of expression profiles--database and tools. Nucleic Acids Res 2005; 33: D562-566.
[19] Cui J, Chen Y, Chou WC, Sun L, Chen L, Suo J, Ni Z, Zhang M, Kong X, Hoffman LL, Kang J, Su Y, Olman V, Johnson D, Tench DW, Amster IJ, Orlando R, Puett D, Li F and Xu Y. An integrated transcriptomic and computational analysis for biomarker identification in gastric cancer. Nucleic Acids Res 2011; 39: 1197-1207.
[20] Cui J, Li F, Wang G, Fang X, Puett JD and Xu Y. Gene-expression signatures can distinguish gastric cancer grades and stages. PLoS One 2011; 6: e17819.
[21] D'Errico M, de Rinaldis E, Blasi MF, Viti V, Falchetti M, Calcagnile A, Sera F, Saieva C, Ottini L, Palli D, Palombo F, Giuliani A and Dogliotti E. Genome-wide expression profile of sporadic gastric cancers with microsatellite instability. Eur J Cancer 2009; 45: 461-469.
[22] Park JH, Park J, Choi JK, Lyu J, Bae MG, Lee YG, Bae JB, Park DY, Yang HK, Kim TY and Kim YJ. Identification of DNA methylation changes associated with human gastric cancer. BMC Med Genomics 2011; 4: 82.
[23] Benjamini Y HY. Controlling the False Discovery Rate: A Practical and Powerful Approach to Multiple Testing. Journal of the Royal Statistical Society Series B (Methodological) 1995; 57: 289-300.
[24] Chen Y, Choong LY, Lin Q, Philp R, Wong CH, Ang BK, Tan YL, Loh MC, Hew CL, Shah N, Druker BJ, Chong PK and Lim YP. Differential Expression of Novel Tyrosine Kinase Substrates during Breast Cancer Development. Mol Cell Proteomics 2007; 6: 2072-2087.
[25] Chong PK, Lee H, Loh MC, Choong LY, Lin Q, So JB, Lim KH, Soo RA, Yong WP, Chan SP, Smoot DT, Ashktorab H, Yeoh KG and Lim YP. Upregulation of plasma C9 protein in gastric cancer patients. Proteomics 2010; 10: 3210-3221.
[26] Chong PK, Lee H, Zhou J, Liu SC, Loh MC, So JB, Lim KH, Yeoh KG and Lim YP. Reduced plasma APOA1 level is associated with gastric tumor growth in MKN45 mouse xenograft model. J Proteomics 2010; 73: 1632-1640.
[27] Yang Y, Lim SK, Choong LY, Lee H, Chen Y, Chong PK, Ashktorab H, Wang TT, Salto-Tellez M, Yeoh KG and Lim YP. Cathepsin S Mediates Gastric Cancer Cell Migration and Invasion via a Putative Network of Metastasis-Associated Proteins. J Proteome Res 2010; 9: 6801.
[28] Hanahan D and Weinberg RA. The hallmarks of cancer. cell 2000; 100: 57-70.
[29] Vander Heiden MG, Cantley LC and Thompson CB. Understanding the Warburg effect: the metabolic requirements of cell proliferation. Science 2009; 324: 1029-1033.
[30] Warburg O. On the origin of cancer cells. Science 1956; 123: 309-314.
[31] Schell JC and Rutter J. The long and winding road to the mitochondrial pyruvate carrier. Cancer Metab 2013; 1: 6.
[32] Ward Patrick S and Thompson Craig B. Metabolic Reprogramming: A Cancer Hallmark Even Warburg Did Not Anticipate. Cancer Cell 2012; 21: 297-308.
[33] Sonveaux P, Végran F, Schroeder T, Wergin MC, Verrax J, Rabbani ZN, De Saedeleer CJ, Kennedy KM, Diepart C and Jordan BF. Targeting lactate-fueled respiration selectively kills hypoxic tumor cells in mice. J Clin Invest 2008; 118: 3930-42.
[34] Pavlides S, Tsirigos A, Vera I, Flomenberg N, Frank PG, Casimiro MC, Wang C, Fortina P, Addya S and Pestell RG. Loss of stromal caveolin-1 leads to oxidative stress, mimics hypoxia and drives inflammation in the tumor microenvironment, conferring the "reverse Warburg effect": a transcriptional informatics analysis with validation. Cell Cycle 2010; 9: 2201-2219.
[35] Gatenby RA and Gillies RJ. Why do cancers have high aerobic glycolysis? Nat Rev Cancer 2004; 4: 891-899.
[36] Fulda S, Galluzzi L and Kroemer G. Targeting mitochondria for cancer therapy. Nat Rev Drug Discov 2010; 9: 447-464.